N-Type Colloidal-Quantum-Dot Solids for Photovoltaics

*David Zhitomirsky, Melissa Furukawa, Jiang Tang, Philipp Stadler, Sjoerd Hoogland, Oleksandr Voznyy, Huan Liu, and Edward H. Sargent**

Colloidal quantum dots (CQDs) are attractive materials for optoelectronic applications due to their low cost, facile processing, and size-dependent bandgap tuning. To form a film capable of electronic transport, nanocrystals that are initially passivated by long hydrocarbon ligands (e.g., oleic acid used in synthesis) are deposited onto a substrate and then treated using short ligands with characteristic functional groups (e.g., dithiols). These displace the long insulating ligands and bring the nanoparticles closer together and into electrical communication with one another.[1] Changing the ligand in this manner also changes the surface passivation and, potentially, the doping of the nanoparticle film in a manner that will depend on the processing environment,[2,3] ligand end-functional group, and the electronic properties of the ligand molecule itself.[4,5]

To date, all photovoltaic devices employing CQD films have primarily relied on p-type conduction in the quantum-dot solid.[6–10] This has mandated combining the p-type light-absorbing materials with an optically transparent n-type electrode such as TiO_2 in order to form a rectifying junction and efficient photovoltaic devices.[11]

We took the view that if photovoltaic-capable CQD solids could also be tailored to have an n-type character, new combinations of materials and attractive new device architectures would become possible. Employing the n-type layer in a CQD photovoltaic device would obviate the need for a high-temperature-sintered TiO_2 electrode, allowing for solution-phase processing at room temperature. In contrast to present architectures, such a p-n homojunction device would be able to absorb solar photons and thus generate and collect photocharges efficiently on both sides of the junction. A quantum-tuned homojunction would overcome another drawback of existing CQD solar cell architectures: depleted-heterojunction devices rely on careful tailoring of the band offset between the p-type solid and the electron acceptor.[12] This implies that the electrode must be reoptimized when quantum size-effect tuning is exploited in the absorbing layer. In contrast, the capability, presented herein, to produce an efficient photovoltaic n-type layer, enabling quantum-tuned homojunction formation, entails inherent matching between the energy levels of the materials on each side of a size-tuned heterojunction.[13] This offers a particularly straightforward route towards tandem and multijunction cells.[14]

In bulk materials, metal-chalcogen binary compound semiconductors are prone to be n-type when off-stoichiometric with a cation metal excess.[15] PbS CQDs have widely been observed to exhibit a lead excess – a consequence of the synthetic protocol in which the co-ordinating ligand binds only the cation and not the anion.[16] Through careful engineering of the nanocrystal surface, we sought to retain the inherent n-type quality of the PbS CQDs.

Hydrazine treatment has previously been reported to convert PbSe CQD films from p- to n-type,[17] and substitutional dopants introduced during synthesis have led to n-type InP and InAs quantum dots.[18] In none of these reports, however, has photovoltaic device operation been reported. Forming an n-type film would require a means of protecting the nanocrystal surfaces from oxygen – a well-known acceptor in bulk PbS[19] and in PbS CQD films.[20] As a first step, this would evidently demand processing in an inert ambient. However, interestingly, taking this step alone when working with Pb-rich PbS nanoparticles passivated using commonly employed organic ligands such as thiols does not result in n-type behavior, but produces ambipolar characteristics[21] (i.e., an intrinsic semiconductor).

Because organic ligands are sterically large, their ability to cover each surface site on a nanoparticle is imperfect. This limits the organic ligands' capacity to protect oxidation-prone nanoparticle surfaces from oxidative attack, even in a <80 ppm O_2 glovebox. We believed that such trace levels of oxygen can induce traps that may pin the Fermi level[22,23] near the midgap, preventing substantial net doping.

We posited that small atomic ligands (Cl^-, Br^- and I^-) recently reported[6] might, with significant further advances, lead to high surface coverage of otherwise-exposed nanoparticle surface sites. This would protect against oxidative attack and enable wide-ranging doping, including significant net n-type doping, of CQD solids. We were also attracted to halogen ions since, if they could participate in substitutional replacement of the chalcogen, they would be expected to provide an additional influence in favor of n-type doping,[24,25] as suggested by theoretical simulations.[26] In these simulations, such substitutional doping was predicted to provide one extra electron without introducing traps in the bandgap.

We fabricated PbS CQD films by replacing long organic ligands with ultrasmall inorganic ones in an inert environment. We employed tetrabutylammonium iodide (TBAI) in methanol

D. Zhitomirsky, M. Furukawa, Dr. P. Stadler,
Dr. S. Hoogland, Dr. O. Voznyy, Prof. E. H. Sargent
Department of Electrical and Computer Engineering
University of Toronto
10 King's College Road, Toronto, Ontario, M5S 3G4, Canada
E-mail: ted.sargent@utoronto.ca
Prof. J. Tang
Wuhan National Laboratory for Optoelectronics
Huazhong University of Science and Technology
1037 Luoyu Rd., Wuhan, Hubei 430074, China
Prof. H. Liu
Department of Electronic Science and Technology
Huazhong University of Science and Technology
1037 Luoyu Rd., Wuhan, Hubei 430074, China

DOI: 10.1002/adma.201202825

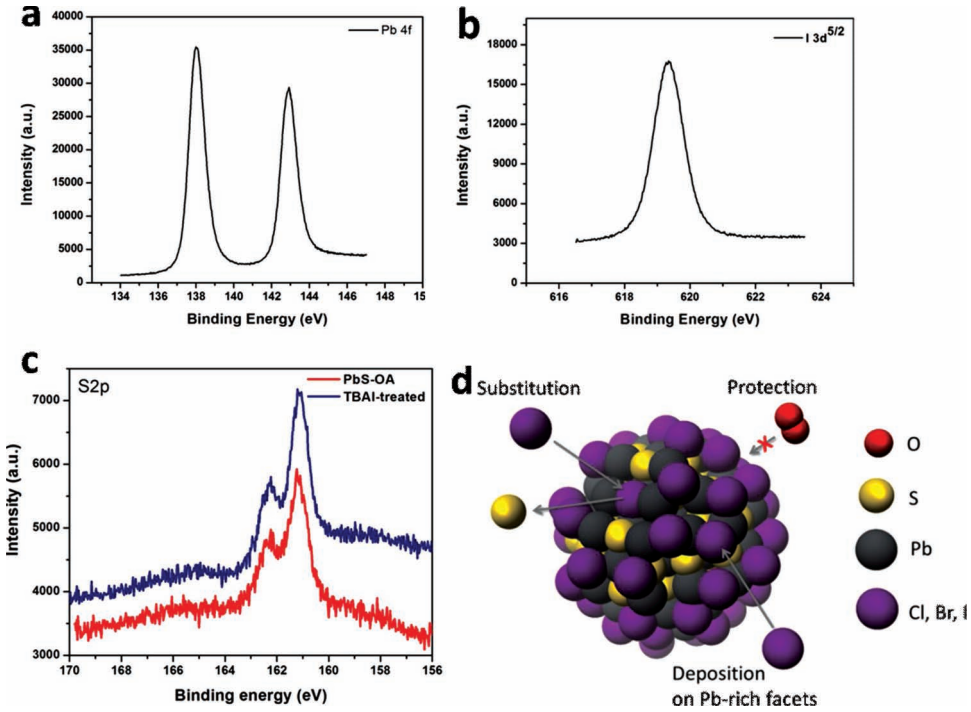

Figure 1. XPS spectra for: a) lead and b) iodine showing the presence of the lead–iodine bond. c) XPS of the sulfur peak showing the absence of sulfur oxides signal. d) Cartoon depiction of the processes that occur as a result of the iodide treatment, either as passivation or substitution.

as a ligand to yield conducting CQD films. Absorption measurements showed that the excitonic features of the CQDs were preserved in the film (Supporting Information, Figure S1). X-ray photoelectron spectroscopy (XPS) elemental analysis of the iodide-treated film showed the appearance of a considerable iodide concentration in the form of a Pb–I bond (**Figure 1**a,b). The iodide treatments remove the original oleate ligand and introduce I^- onto the PbS CQD's surface. This allows the passivation of the surface dangling bonds associated with the previously unpassivated surface cations sites,[6] and provides protection from trace oxygen (Figure 1c, Supporting Information, Figure S2); iodine substitution for sulfur may further move the nanocrystal film towards being n-type (Figure 1d).

We constructed thin-film field-effect transistors (FETs) to characterize the doping type and transport behavior in these films. The device structure (**Figure 2**a) consisted of an aluminum/aluminum oxide gate, octadecyl trichlorosilane surfactant, the PbS CQD film and titanium source and drain electrodes. The device exhibited an n-type transfer response (Figure 2b) with an on/off ratio of 10^5 and negligible leakage: when the gate voltage, V_g, was increased from 0 V to 2 V, majority carriers (electrons) accumulated at the Al_2O_3/PbS CQD film interface, forming a highly conductive channel and leading to a significant increase in the drain-source current, I_d. The output characteristics (Figure 2c) showed controlled drain-source channel modulation by the gate. The mobility extracted from this device was 0.1 $cm^2\ V^{-1}\ s^{-1}$ (Supporting Information, S3): this is the highest reported for PbS CQDs.

These results are consistent with the notion that excess Pb is a donor in bulk PbS:[27] indeed, we found that our halide-treated films are lead-rich (Pb:S = 1.35 from XPS measurement), consistent with the proposed stoichiometric mechanism governing the n-type nature of our materials. Hence, by minimizing the ambient oxygen and using high-coverage atomic ligands to protect the surface against any trace quantities of oxygen, we were able to retain the n-type character of our CQDs. We further confirmed that the film remains n-type when tested in argon (Supporting Information, Figure S2), ruling out the possibility that the specific use of a N_2 ambient environment was a contributing factor to the n-doping in the CQD film.[28]

To elucidate the impact of oxygen, we exposed n-type films (Supporting Information, Figure S4) to oxygen, which eventually turned the film p-type after exposure for 10 min, confirming the role of oxygen as the dominant p-dopant. By overwhelming the CQD surface with oxygen, it was possible to overcome the surface protection afforded by the halogen-ion-passivation scheme.

We sought to explore further the role of the halogen ion on the doping. Firstly, we varied the halogen salts, using tetrabutylammonium bromide (TBAB) and tetrabutylammonium chloride (TBAC). Both the average carrier density and mobility (**Figure 3**a) depend strongly on the species of halogen used in passivation. The iodide-passivated film has the lowest doping density and the highest carrier mobility, while the chloride-treated film has the highest carrier density and the lowest mobility. Depending on the application, it would be possible to take advantage of this 10^{16} to 10^{18} cm^{-3} doping range simply by changing the type of halogen ion. We found experimentally that iodide was the most advantageous halide treatment for photovoltaic applications, as it produces a high mobility and a low

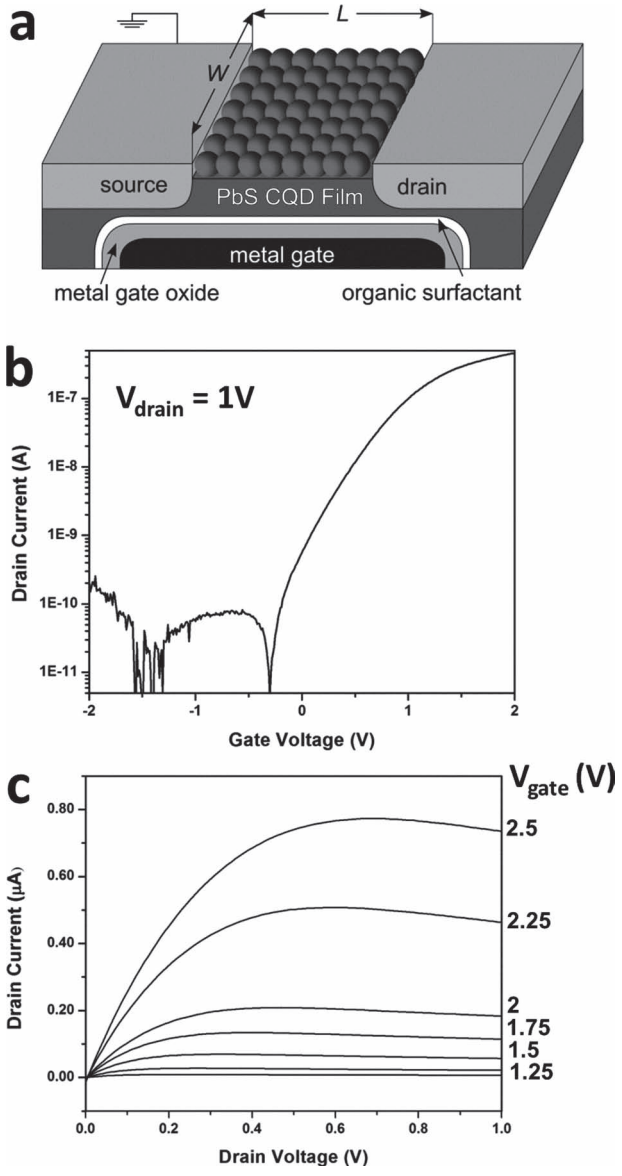

Figure 2. a) FET, including an aluminum/aluminum oxide gate, PbS CQD film, and Ti source and drain contacts. b) n-type response generated by the FET as a result of a conducting electron channel. c) Output characteristics of the FET, showing gate modulation of the channel across several voltages.

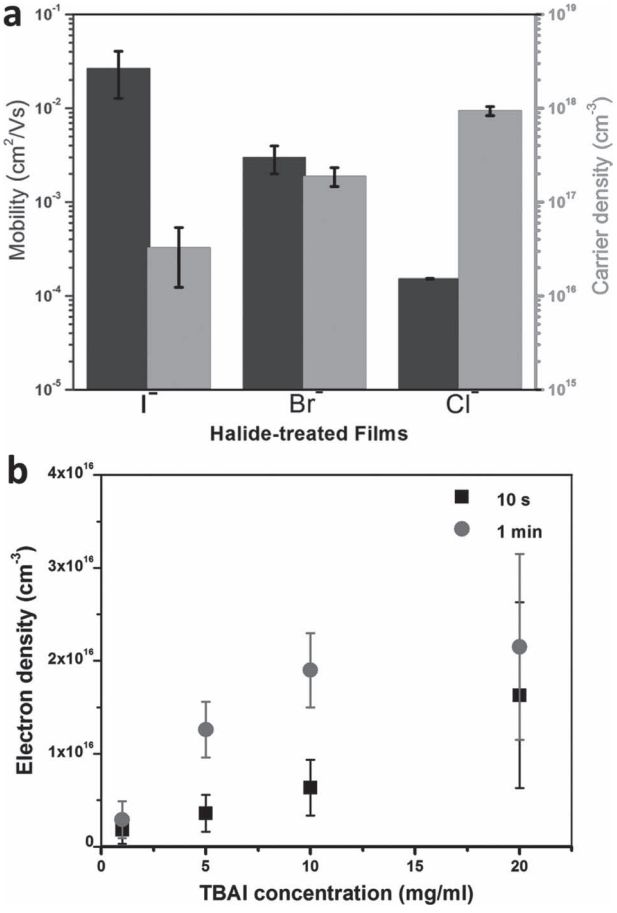

Figure 3. a) Doping densities (grey) and mobilities (black) achieved by treating the PbS CQDs with different halogen ions. b) The variation in doping density observed as the concentration and treatment time with iodine was varied between 1 min and 10 s, as well as 1 mg ml^{-1} to 20 mg ml^{-1} concentrations.

doping density, such as to allow better carrier collection and greater depletion of the active absorbing layer, respectively. We sought to probe our iodide process further, and fabricated films under different treatment conditions by varying the treatment time and the treatment concentration. We found that the doping density increases in proportion to the product of treatment time and concentration, consistent with an increasing quantity of iodide being incorporated into the film (Figure 3b). This again is consistent with iodine ions substituting for sulfur, analogous to their role in bulk metal chalcogenides. XPS confirmed the increased quantity of iodine in the films as the treatment conditions were varied, with the iodine peak growing (Supporting Information, Figure S5), while the lead peak remained almost constant. Thus, the halogen ion was shown to act as an excellent passivating agent, as well as having the capability of n-type doping the film through substitution.

We sought to showcase our n-type CQD solids in an operating photovoltaic device. FET studies have revealed both n and p-type modulation in InAs[29] and CdSe[30] CQD films, with the same aim stated herein, of providing an avenue to p-n junction devices; however, no such devices have previously been reported. The promise of our halogen-ion strategy in enabling the first all-CQD p-n junction device lies in the previously established low trap-state density in halogen-ion-passivated CQD films.[6] We built devices consisting of indium tin oxide (ITO) on glass with a highly doped p-type CQD film on top; a much thicker n-type CQD layer formed the principal light absorber interfacing with the p-layer; the n-layer was contacted using a shallow-work-function Al metal top electrode which had proved to be ohmic to our n-type film. From the strong rectification of the ITO:pPbS:nPbS:Al device (Supporting Information, Figure S6), we conclude that the p-n junction is the source of rectification. The resultant photovoltaic devices provided 5.4%[13] solar power conversion efficiency under AM1.5

illumination, a substantial advance relative to the best previously reported all-solution-processed, all-room-temperature-processed p-n devices, which employed one bulk n-type layer and one quantum-confined p-type layer.[31]

In conclusion, we have demonstrated a chemically controllable method of forming n-type CQD films that are efficient in photovoltaic capture. The films combine high carrier mobilities with wide-ranging control over net doping. We achieve this by combining the excellent surface passivation and substitutional doping provided by halide anions. The resultant capability of producing both p-type and n-type CQD films, and combining them together, opens avenues to quantum junction p-n devices, as well as bipolar transistors and thyristors.

Experimental Section

Materials Preparation: PbS CQDs of various sizes were fabricated following a modified published recipe.[32] The CQDs were precipitated using distilled acetone twice and anhydrous methanol once, and dispersed in octane at a concentration of 25 mg ml^{-1} and stored inside the glovebox for future use.

Film Deposition: Layer-by-layer spin-coating was applied to fabricate the CQD film. Deposition of the n-layer was carried out inside the glovebox: 1) 4 drops of PbS CQDs in octane (25 mg ml^{-1}) were dropped onto FET substrates and were spin-cast at 2500 rpm for 10 s; 2) 0.75 ml of 10 mg ml^{-1} TBAI in methanol solution were deposited, soaked for 1 min, and this was followed by spin-coating for 10 s at 2500 rpm; 3) 0.75 ml of methanol were dropped and spin-cast at 2500 rpm for 10 s (repeated twice). A final film thickness of 2 such layers was used for the FET devices.

FET Measurement: The FET structures used herein employed a high-ε gate dielectric. These were made by physical vapor deposition (PVD) of Al onto a glass substrate, followed by electrochemical anodization to form an 8 nm gate oxide. Octadecyl trichlorosilane was used as passivating surfactant. The films were prepared by spin-coating and solid-state ligand exchange. Titanium was employed as the top contact. The completed FET device had a channel length of 33 μm and a channel width of 2 mm. FET measurements were performed inside a N_2 glovebox. For oxygen vs. nitrogen measurements, commercial silicon wafers (highly doped p-type using boron) with a thin layer of thermally oxidized SiO_2 were used as the substrate and gate dielectric. Au and Al (or Ag) were used as the source and drain electrodes to form the ohmic contact to the p-type and n-type materials, respectively. For the bottom-contact FET studies, prepatterned Au contacts were used with a channel length of 5 μm and channel width of 1 mm. Top-contact FET devices employed thermal evaporation of Al or Ag through a shadow mask to create channel lengths of 25 and 50 μm and channel widths of 0.5 and 1 mm. A typical CQD film thickness for the FET studies was 40 nm.

XPS: The surface elements and chemical states of PbS CQDs were examined using X-ray photoelectron spectroscopy (XPS) (PHI-5500) with a monochromated Al K radiation source (1486.7 eV) to excite photoelectrons in an ultrahigh vacuum atmosphere at $\approx 10^{-9}$ Torr. The binding-energy scale was calibrated using the Au $4f_{7/2}$ peak to 83.98 eV and the Cu $2p_{3/2}$ peak of sputter-cleaned Cu to 932.67 eV.

PCE Characterization: The current–voltage characteristics were measured using a Keithley 2400 source-meter in a N_2 ambient environment. The solar spectrum at AM1.5 was simulated to within class A specifications (less than 25% spectral mismatch) with a Xe lamp and filters (Solar Light Company Inc.) with a measured intensity at 100.6 mW cm^{-2}. The source intensity was measured using a Melles–Griot broadband power meter and a Thorlabs broadband power meter through a circular 0.05 cm^2 aperture at the position of the device and confirmed with a calibrated reference solar cell (Newport, Inc.). The accuracy of the power measurement was estimated to be ±5%.

Supporting Information

Supporting information is available from the Wiley Online Library or from the author.

Acknowledgements

We thank Angstrom Engineering and Innovative Technology for useful discussions regarding material-deposition methods and control of the glovebox environment, respectively. The authors would like to acknowledge the technical assistance and scientific guidance of E. Palmiano, R. Wolowiec, and D. Kopilovic. This publication is based, in part, on work supported by Award KUS-11-009-21, made by King Abdullah University of Science and Technology (KAUST), by the Ontario Research Fund Research Excellence Program, and by the Natural Sciences and Engineering Research Council (NSERC) of Canada. D.Z. acknowledges financial support through the NSERC CGS D Scholarship.

Received: July 12, 2012
Revised: August 16, 2012
Published online: September 12, 2012

[1] K. J. Williams, W. A. Tisdale, K. S. Leschkies, G. Haugstad, D. J. Norris, E. S. Aydil, X.-Y. Zhu, *ACS Nano* **2009**, *3*, 1532–1538.
[2] R. Debnath, J. Tang, D. A. Barkhouse, X. Wang, A. G. Pattantyus-Abraham, L. Brzozowski, L. Levina, E. H. Sargent, *J. Am. Chem. Soc.* **2010**, *132*, 5952–5953.
[3] G. Konstantatos, I. Howard, A. Fischer, S. Hoogland, J. Clifford, E. Klem, L. Levina, E. H. Sargent, *Nature* **2006**, *442*, 180–183.
[4] H. Zhang, B. Hu, L. Sun, R. Hovden, F. W. Wise, D. A. Muller, R. D. Robinson, *Nano Lett.* **2011**, *11*, 5356–5361.
[5] K. S. Jeong, J. Tang, H. Liu, J. Kim, A. W. Schaefer, K. Kemp, L. Levina, X. Wang, S. Hoogland, R. Debnath, L. Brzozowski, E. H. Sargent, J. B. Asbury, *ACS Nano* **2011**, *6*, 89–99.
[6] J. Tang, K. W. Kemp, S. Hoogland, K. S. Jeong, H. Liu, L. Levina, M. Furukawa, X. Wang, R. Debnath, D. Cha, K. W. Chou, A. Fischer, A. Amassian, J. B. Asbury, E. H. Sargent, *Nat. Mater.* **2011**, *10*, 765–771.
[7] J. Gao, J. M. Luther, O. E. Semonin, R. J. Ellingson, A. J. Nozik, M. C. Beard, *Nano Lett.* **2011**, *11*, 1002–1008.
[8] K. S. Leschkies, T. J. Beatty, M. S. Kang, D. J. Norris, E. S. Aydil, *ACS Nano* **2009**, *3*, 3638–3648.
[9] P. R. Brown, R. R. Lunt, N. Zhao, T. P. Osedach, D. D. Wanger, L.-Y. Chang, M. G. Bawendi, V. Bulovi , *Nano Lett.* **2011**, *11*, 2955–2961.
[10] I. J. Kramer, D. Zhitomirsky, J. D. Bass, P. M. Rice, T. Topuria, L. Krupp, S. M. Thon, A. H. Ip, R. Debnath, H.-C. Kim, E. H. Sargent, *Adv. Mater.* **2012**, *24*, 2315–2319.
[11] A. G. Pattantyus-Abraham, I. J. Kramer, A. R. Barkhouse, X. Wang, G. Konstantatos, R. Debnath, L. Levina, I. Raabe, M. K. Nazeeruddin, M. Grätzel, E. H. Sargent, *ACS Nano* **2010**, *4*, 3374–3380.
[12] H. Liu, J. Tang, I. J. Kramer, R. Debnath, G. I. Koleilat, X. Wang, A. Fisher, R. Li, L. Brzozowski, L. Levina, E. H. Sargent, *Adv. Mater.* **2011**, *23*, 3832–3837.
[13] J. Tang, H. Liu, D. Zhitomirsky, S. Hoogland, X. Wang, M. Furukawa, L. Levina, E. H. Sargent, *Nano Lett.* **2012**, DOI:10.1021/nl302436r.
[14] X. Wang, G. I. Koleilat, J. Tang, H. Liu, I. J. Kramer, R. Debnath, L. Brzozowski, D. A. R. Barkhouse, L. Levina, S. Hoogland, E. H. Sargent, *Nat. Photon.* **2011**, *5*, 480–484.
[15] R. S. Allgaier, W. W. Scanlon, *Phys. Rev.* **1958**, *111*, 1029–1037.
[16] W. Ma, J. M. Luther, H. Zheng, Y. Wu, A. P. Alivisatos, *Nano Lett.* **2009**, *9*, 1699–1703.
[17] D. V. Talapin, C. B. Murray, *Science* **2005**, *310*, 86–89.

[18] D. Mocatta, G. Cohen, J. Schattner, O. Millo, E. Rabani, U. Banin, *Science* **2011**, *332*, 77–81.
[19] R. H. Harada, H. T. Minden, *Phys. Rev.* **1956**, *102*, 1258–1262.
[20] G. Konstantatos, L. Levina, A. Fischer, E. H. Sargent, *Nano Lett.* **2008**, *8*, 1446–1450.
[21] T. P. Osedach, N. Zhao, T. L. Andrew, P. R. Brown, D. D. Wanger, D. B. Strasfeld, L.-Y. Chang, M. G. Bawendi, V. Bulovi , *ACS Nano* **2012**, *6*, 3121–3127.
[22] D. Zhitomirsky, I. J. Kramer, A. J. Labelle, A. Fischer, R. Debnath, J. Pan, O. M. Bakr, E. H. Sargent, *Nano Lett.* **2012**, *12*, 1007–1012.
[23] P. Nagpal, V. I. Klimov, *Nat. Commun.* **2011**, *2*, 486.
[24] R. Dalven, *Infrared Phys.* **1969**, *9*, 141–184.
[25] S. H. Kwan, C. G. Colozzi, A. Linz, *J. Appl. Phys.* **1974**, 3273–3276.
[26] H. Peng, J.-H. Song, M. G. Kanatzidis, A. J. Freeman, *Phys. Rev. B: Condens. Matter* **2011**, *84*, 125207.
[27] W. W. Scanlon, R. F. Brebrick, *Physica* **1954**, *20*, 1090–1092.
[28] K. S. Leschkies, M. S. Kang, E. S. Aydil, D. J. Norris, *J. Phys. Chem. C* **2010**, *114*, 9988–9996.
[29] S. M. Geyer, P. M. Allen, L.-Y. Chang, C. R. Wong, T. P. Osedach, N. Zhao, V. Bulovic, M. G. Bawendi, *ACS Nano* **2010**, *4*, 7373–7378.
[30] A. Sahu, M. S. Kang, A. Kompch, C. Notthoff, A. W. Wills, D. Deng, M. Winterer, C. D. Frisbie, D. J. Norris, *Nano Lett.* **2012**, *12*, 2587–2594.
[31] A. K. Rath, M. Bernechea, L. Martinez, G. Konstantatos, *Adv. Mater.* **2011**, *23*, 3712–3717.
[32] M. A. Hines, G. D. Scholes, *Adv. Mater.* **2003**, *15*, 1844–1849.